International Journal of Bifurcation and Chaos, Vol. 11, No. 3 (2001) 801–820

NEWTON'S METHOD AND MORSE INDEX FOR SEMILINEAR ELLIPTIC PDES

JOHN M. NEUBERGER* and JAMES W. SWIFT†
Department of Mathematics and Statistics,
Northern Arizona University P.O. Box 5717,
Flagstaff, AZ 86011-5717, USA

Received April 20, 2000; Revised June 1, 2000

In this paper we primarily consider the family of elliptic PDEs $\Delta u + f(u) = 0$ on the square region $\Omega = (0, 1) \times (0, 1)$ with zero Dirichlet boundary condition. Following our previous analysis and numerical approximations which relied on the variational characterization of solutions as critical points of an "action" functional, we consider Newton's method on the gradient of that functional. We use a Galerkin expansion, in eigenfunctions of the Laplacian, to find solutions of arbitrary Morse index. Taking $f'(0)$ to be a bifurcation parameter, we analyze the bifurcations from the trivial solution, $u \equiv 0$, using symmetry arguments and our numerical algorithm. The Morse index of the approximated solutions is provided and support is found concerning several existence and nodal structure conjectures. We discuss the applicability of this method to find critical points of functionals in general.

1. The Semilinear Problem

The primary equation we consider is a superlinear elliptic zero Dirichlet boundary value problem on a piecewise smooth bounded region $\Omega \subset \mathbf{R}^N$. In this paper's numerical investigations we let $N = 2$ and $\Omega = (0, 1) \times (0, 1)$, but the method can be applied to other regions. Let Δ be the Laplacian operator. We seek solutions to the boundary value problem

$$\begin{cases} \Delta u + f(u) = 0 \text{ in } \Omega \\ u = 0 \text{ on } \partial\Omega. \end{cases} \tag{1}$$

Recall that the eigenvalues of $-\Delta$ with zero Dirichlet boundary condition in Ω satisfy

$$0 < \lambda_1 < \lambda_2 \leq \lambda_3 \leq \cdots \to \infty\,.$$

We designate the corresponding eigenfunctions by $\{\psi_i\}_{i\in\mathbf{N}}$, taken to be normal in $L_2 = L_2(\Omega)$ and of course orthogonal in both the Sobolev space $H = H_0^{1,2}(\Omega)$ and in L_2, with inner products

$$\langle u, v\rangle_H = \int_\Omega \nabla u \cdot \nabla v \, dx \quad \text{and} \quad \langle u, v\rangle_2 = \int_\Omega u\, v \, dx$$

respectively (see [Adams, 1975; Gilbarg & Trudinger, 1983], or [Neuberger, 1997a, 1997b]).

For the PDE (1) on a square region, $\Omega = (0, 1) \times (0, 1)$, it is well known that the (doubly indexed) eigenvalues and eigenfunctions of $-\Delta$ are

$$\lambda_{m,n} = (m^2 + n^2)\pi^2 \quad \text{and}$$
$$\psi_{m,n} = 2\sin(m\pi x)\sin(n\pi y)\,, \tag{2}$$

where m and n range over all positive integers. One of the main goals in this paper is to demonstrate the importance of these eigenfunctions to the theory of our type of PDE in general and to our numerical method in particular.

*E-mail: John.Neuberger@nau.edu
†E-mail: Jim.Swift@nau.edu

Although our numerical method works in general on a much wider class of variational problems, we consider specific assumptions which have led to existence theorems of sign-changing solutions (see [Castro *et al.*, 1997a; Neuberger, 1998; Castro *et al.*, 1997b; Castro *et al.*, 1998]). In this paper we focus on the case where f is superlinear and subcritical, as per the hypothesis of Theorem 2.2 below. We wish to emphasize that although infinitely many solutions have been proven to exist for various special cases, e.g. when $N = 1$, f is odd, or Ω is a ball in $\mathbf{R}^N$, in the general case of Theorem 2.2 only three nontrivial solutions are currently proven to exist.

Let $F(u) = \int_0^u f(s)\,ds$ for all $u \in \mathbf{R}$ define the primitive of f. We then define the action functional $J : H \to \mathbf{R}$ by

$$J(u) = \int_\Omega \left\{ \frac{1}{2}|\nabla u|^2 - F(u) \right\} dx\,. \tag{3}$$

We will make assumptions on f so that J is well defined and of class C^2 on H. The directional derivative of J at u in the v direction is defined to be

$$J'(u)(v) = \lim_{t\to 0} \frac{J(u+tv) - J(u)}{t}\,,$$

and the second derivative $J''(u)(v,\, w)$ is similarly defined. A calculation shows

$$J'(u)(v) = \int_\Omega \{\nabla u \cdot \nabla v - f(u)v\}\,dx \tag{4}$$

and

$$J''(u)(v,\, w) = \int_\Omega \{\nabla v \cdot \nabla w - f'(u)v\,w\}\,dx\,. \tag{5}$$

If u is C^2, then we can do integration by parts on (4) to get

$$J'(u)(v) = -\int_\Omega \{\Delta u + f(u)\}v\,dx\,. \tag{6}$$

Therefore, a classical solution to the PDE (1) is a critical point of J. (A critical point of J is a function u such that $J'(u)(v) = 0$ for all v.) By definition, critical points of J are weak solutions to (1) (see [Rabinowitz, 1986]). By regularity theory for elliptic boundary value problems (see [Gilbarg & Trudinger, 1983]), u is a classical solution to our superlinear problem (under the exact hypothesis below) if and only if u is a weak solution to (1). In other words, critical points of the action functional J are precisely the classical solutions of the PDE we consider in this paper.

For a solution of the PDE, it is natural to ask if the critical point is a local minimum, a local maximum, or a saddle point of J. For a broad class of functions f, every solution to the PDE (1) has an infinite number of orthogonal directions in function space where J "curves up" (i.e. $J''(u)(v,\, v) > 0$), and a finite number where J "curves down." Roughly speaking, the Morse index is the number of linearly independent directions in function space in which J "curves down." (See Sec. 2.3 for a definition of the Morse index, or see [Milnor, 1963] for a detailed discussion.) Thus, a solution that is a local minimum of J has Morse index 0. All other solutions to the PDE (1) are saddle points, since no solutions are local maxima of J.

It is often instructive to keep in mind the reaction–diffusion equation

$$u_t = \Delta u + f(u)\,. \tag{7}$$

In this paper, we are searching for the stationary (time-independent) solutions to this reaction–diffusion equation. In this context, the Morse index is the number of unstable directions of the stationary solution.

2. Low-Morse Index Solutions

2.1. *Variational existence proofs*

A starting point for analytical investigation can be found in the following theorem, proven in [Castro *et al.*, 1997]. Although our numerical scheme can certainly be used to attack different problems where existence results may or may not yet found be, let us give the precise hypothesis under which Theorem 2.2 is known to hold.

In particular, we take $f \in C^1(\mathbf{R}, \mathbf{R})$ such that $f(0) = 0$. We assume that there exist constants $A > 0$ and $p \in (1,\, N + 2/N - 2)$ such that $|f'(u)| \le A(|u|^{p-1} + 1)$ for all $u \in \mathbf{R}$. It follows that f is *subcritical*, i.e. there exists $B > 0$ such that $|f(u)| \le B(|u|^p + 1)$. For $N = 1$ this condition is omitted, while for $N = 2$ it suffices to have $p \in (1,\, \infty)$ (see [Rabinowitz, 1986]). Also, we assume that there exists $m \in (0,\, 1)$ such that

$$\frac{m}{2} f(u)u \ge F(u)\,, \tag{8}$$

(in fact this need only hold for $|u| > \rho$ for some $\rho > 0$), and that f is *superlinear*, i.e.

$$\lim_{|u|\to\infty} \frac{f(u)}{u} = \infty\,. \tag{9}$$

Finally, we make the assumption that f satisfies

$$f'(u) > \frac{f(u)}{u} \quad \text{for} \quad u \neq 0\,. \tag{10}$$

For convenience, we will call (1) with all of the above conditions on f "the superlinear problem". Recall that subcritical growth and the Sobolev Embedding Theorem (see [Adams, 1975]) imply that H is compactly embedded into L_{p+1}, which in turn shows that J is well defined on all of H. Under our full hypothesis, J is in fact twice differentiable on H (see [Rabinowitz, 1986]).

Theorem 2.2. (The CCN Theorem [Castro *et al.*, 1997]). *If $f'(0) < \lambda_1$, then the superlinear problem (1) has at least three nontrivial solutions: $\omega_1 > 0$ in Ω, $\omega_2 < 0$ in Ω, and ω_3. The function ω_3 changes sign exactly once in Ω, i.e. $(\omega_3)^{-1}(\mathbf{R} - \{0\})$ has exactly two connected components. If nondegenerate, the one-sign solutions are Morse index (MI) 1 critical points of J, and the sign-changing solution has MI 2. Furthermore,*

$$J(\omega_3) \geq J(\omega_1) + J(\omega_2)\,.$$

For convenience, we call ω_3 the CCN solution. In this $f'(0) < \lambda_1$ superlinear case, the trivial solution $u = 0$ has MI 0 and is the only local minimum of J. All other critical points (solutions to (1)) are saddle points.

To see how these three low MI solutions can be found, we first define $u_+ = \max_\Omega\{u, 0\}$ and $u_- = \min_\Omega\{u, 0\}$. See [Castro *et al.*, 1997] (or more fundamentally [Kinderlehrer & Stampacchia, 1979]) for important properties of the continuous map $u \to u_+$ from H (and $L_{p+1}(\Omega)$) into itself. Then we construct two important subsets of H:

$$S = \{u \in H - \{0\} : J'(u)(u) = 0\}$$

and

$$S_1 = \{u \in S : u_+ \in S,\, u_- \in S\}\,.$$

In fact, S is a submanifold diffeomorphic to the unit sphere in H. To find MI 1 one-sign solutions, one need only find minimizers of $J|_S$, and to find sign-changing exactly-once MI 2 solutions, one seeks minimizers of $J|_{S_1}$. In [Castro *et al.*, 1997] we provide existence proofs for both of these types of solutions while in [Neuberger, 1997a, 1997b] we construct a numerical algorithm for approximating them.

If we relax the assumption that $f'(0) < \lambda_1$, the set S is not a manifold. Proving that the sign-changing solution found in [Castro *et al.*, 1997] persists when $f'(0) \in [\lambda_1, \lambda_2)$ is an effort currently in progress. Problems of this sort suggest that one let $\lambda = f'(0)$ vary as a bifurcation parameter. A key idea in this paper is that the eigenfunctions of $-\Delta$ form a basis for H and L_2 and that finite dimensional representations of u, $\nabla J(u)$, and $D^2J(u)$ in H or L_2 can be written as vectors and matrices with this coordinate choice. This suggests our Galerkin-type approach in Sec. 3.

Our success at constructing a substantial portion of the bifurcation diagram for the superlinear problem is a major achievement of this paper, although we hope that the utility of our numerical method for other problems is also of general interest. Ultimately, we seek to prove the existence and describe the nodal structure of all solutions to the superlinear problem (and indeed the PDE (1) with other types of nonlinearities). As a first attempt to do so, we need tools for obtaining higher MI solutions. We hope that our numerical method, which can in principle find all solutions, will suggest methods of proof for the existence and nodal structure of said solutions. Certainly, the numerical experiments can support or refute new and old conjectures.

2.2. *Function spaces, inner products and gradients*

Making the correct choice of space and inner product is always important when using the variational method. Although theory tells us that the so-called weak solutions in H are in fact in C^2, it is necessary to use the Hilbert space H as the domain of the functional J in order to find existence proofs. When considering steepest descent methods, it is essential that one not use the poorly performing L_2 gradient.

One defines the Sobolev gradient as the unique function $z = \nabla_H J(u)$ satisfying $J'(u)(v) = \langle z, v\rangle_H$. From Eq. (4) we get

$$\nabla_H J(u) = u + \Delta^{-1} f(u)\,. \tag{11}$$

If in addition $u \in C^2$, the "usual" L_2 gradient $w = \nabla_2 J(u)$ exists and uniquely satisfies $J'(u)(v) = \langle w, v\rangle_2$. From Eq. (6) we get

$$\nabla_2 J(u) = -\Delta u - f(u)\,.$$

Hence, if $\nabla_2 J(u)$ exists for some $u \in L_2$, then the two gradients are related by $\nabla_2 J(u) = -\Delta(\nabla_H J(u))$.

It is generally felt among numerical analysts that steepest descent is an inferior method due to sluggish performance. This is in fact true if one uses the L_2 gradient, which is only densely defined. The finite dimensional approximation of this "usual" gradient often attempts to approximate something which does not exist! Steepest descent is quite effective, however, when one uses the Sobolev gradient which is defined on all of H. We highly recommend [Neuberger, 1997a, 1997b] for all matters concerning Sobolev gradients and differential equations.

We will be restricting our approximations to a finite dimensional subspace G of L_2 consisting of twice continuously differentiable functions. That is to say, the L_2 gradient $\nabla_2 J(u)$ will exist for all $u \in G$. More importantly, the two gradients $\nabla_2 J(u)$ and $\nabla_H J(u)$ perform identically when Newton's method is used to find a critical point. To see this fact, first note that the Hessians (self-adjoint bilinear operators) satisfy

$$J''(u)(v, w) = \langle D_H^2 J(u)v, w\rangle_H = \langle D_2^2 J(u)v, w\rangle_2 ,$$

for all u, v and w in G. Then since $-\Delta D_H^2 J(u) = D_2^2 J(u)$ for all $u \in G$, we have the identical Newton search directions $(D_H^2 J(u))^{-1}\nabla_H J(u) = (D_2^2 J(u))^{-1}\nabla_2 J(u)$. In our new Galerkin approach we use the L_2 inner product, norm, gradient, and Hessian; henceforth we drop the subscript "2" when referring to any L_2 expression. The Newton iteration can then be written as

$$u_{k+1} = u_k - (D^2 J(u_k))^{-1}\nabla J(u_k) . \qquad (12)$$

We will see that this scheme can be used to find many high MI solutions.

The Morse index of a solution u is defined when $D^2 J(u)$ has no zero eigenvalues, in which case the MI is the (finite) number of negative eigenvalues. For convenience, we generally say in this paper that a solution u has MI k if $D^2 J(u)$ has k negative eigenvalues. It is understood that this is only strictly true if one knows that the solution is *non-degenerate*, i.e. the Hessian is invertible. For completeness, we now briefly describe a previous low MI scheme.

2.3. *Numerical scheme for MI 1 and MI 2 solutions*

A numerical method (see [Neuberger, 1997a, 1997b]) for finding the solutions suggested by Theorem 2.2 is to find Morse Index (MI) 1 and 2 solutions by minimax, that is finding minimizers of $J|_S$ and $J|_{S_1}$ by a combination of maximizing in one or two directions to stay on S or S_1 and doing steepest descent in all other directions. Since under the hypothesis of Theorem 2.2 the set S is a manifold, we can use the facts that

$$\text{given } u \neq 0 \text{ there exists a unique } \hat{\alpha} > 0$$
$$\text{such that } \hat{\alpha}u \in S$$

and that

$$J(\hat{\alpha}u) = \max_{\alpha>0} J(\alpha u)$$

to project nonzero elements of H on to S and sign-changing elements of H on to S_1. From (11) we see that the Sobolev gradient $\nabla_H J(u)$ can be computed by solving a system via standard algorithms. With this gradient in hand, descent steps can be taken to obtain minimizers of $J|_S$ and $J|_{S_1}$.

The above one-sign algorithm, although independently discovered and published in [Neuberger, 1997a, 1997b], is in fact an application of the celebrated Mountain Pass Algorithm (MPA) due to Choi and McKenna [1993]. The sign-changing algorithm (see also [Neuberger, 1997a, 1997b]), which uses the splitting into positive and negative parts in order to gain membership to S_1, has recently been called the Modified Mountain Pass Algorithm (MMPA) (see [Costa *et al.*, 1999]). Of course the MMPA fails to converge to any critical point of MI greater than 2, just as the MPA fails to find critical points of MI greater than 1.

So what does one do to find higher Morse index solutions? At this time we do not know of higher codimension sets analogous to S and S_1 onto which we may project iterates. Indeed, if we had such sets if would be likely that we have the theory to prove the existence of many more solutions! One scheme we have tried successfully (see [Neuberger, 1997]), if not efficiently, is to find global minimizers of the functional ϕ defined by

$$\phi(u) = \frac{1}{2}||\nabla_H J(u)||_2^2 .$$

Obviously all critical points of J are now zeroes of the non-negative functional ϕ. We omit the technical details and suggest [Neuberger, 1997a, 1997b] as a reference for this and other steepest descent

techniques. The potential exists for doing analysis on the behavior of ϕ (similar to that done on J in [Castro *et al.*, 1997] and elsewhere) which might well lead to existence proofs.

Our new algorithm as outlined in the following section is in a sense weighted steepest descent coupled with "appropriate" projections similar to P_S and P_{S_1}. That Newton's method automatically picks out these projections to find minimax solutions of arbitrary MI is a wonderful phenomenon.

3. Newton's Method and Morse Index

3.1. *Solver for general nonlinearities*

For convenience, we call our method the "Gradient Newton Galerkin Algorithm" (GNGA). It is a Galerkin method in the sense that a finite subbasis of orthonormal functions is used to work with Fourier type approximations. Newton's method is used to find zeroes of finite dimensional approximations to ∇J. Certainly Newton–Galerkin methods have been developed and used by others (see e.g. [Argyros, 1997] and references therein.)

To the best of our knowledge this is the first time such a method has used eigenfunctions of the Laplacian as the Galerkin-basis and sought zeroes of the gradient of a nonlinear functional as a means for finding solutions to elliptic Dirichlet problems. For regions other than those where the eigenfunctions are known in closed form there will be a substantial effort required to generate the basis. This effort will only have to be done once for each given region and eliminates the need for numerical differentiation when computing Newton search directions. Our initial efforts were in *Mathematica*, where short simple codes found fairly accurate low-energy low-Morse index solutions to the superlinear problem on the square. Subsequent efforts used either FORTRAN and many more Fourier modes or *Mathematica* and specialized polynomial code to find high-energy high-Morse index solutions and accurate symmetry-bifurcation data. Without question, the technique can be applied to a much wider range of problems.

We denote the number of negative eigenvalues of a (finite or infinite dimensional) bilinear operator A by $\mathrm{sig}(A)$ (signature). Note that if u is a nondegenerate solution to (1), i.e. $D^2J(u)$ is invertible, then $\mathrm{sig}(D^2J(u))$ is the MI of u. In [Neuberger, 1997a, 1997b] as outlined in the previous section, one can find MI 1 and 2 solutions to (1) by doing steepest descent steps coupled with steepest *ascent* steps in the u direction (to minimize $J|_S$) or in the u_+ and u_- directions (to minimize $J|_{S_1}$). To see why this works, first note that

$$J''(u)(v,\, v) = ||v||_H^2 - \int_\Omega f'(u)v^2\, dx\,,$$

and so by (10) and for $v \in S$ we have

$$J''(v)(v,\, v) = ||v||_H^2 - \int_\Omega f'(v)v^2\, dx < ||v||_H^2 - \int_\Omega f(v)v\, dx = J'(v)(v) = 0\,.$$

That is to say, J is "concave down" in the v direction for any $v \in S$. If, in addition, $v \in S_1$, then J is concave down in two orthogonal directions $v_\pm$, since

$$J''(v)(v_\pm,\, v_\pm) = J''(v_\pm)(v_\pm,\, v_\pm) < 0\,.$$

(The equality holds for all v, by the definition of $v_\pm$ and Eq. (5), and the inequality holds since $v_\pm \in S$.)

To generalize this idea for finding saddle points by maximizing infinitely many concave down directions and minimizing in the remaining cofinite directions, we consider the eigenfunctions of the Hessian $h = D^2J(u)$ corresponding to negative eigenvalues. That is to say, we can in theory know the directions in which J is concave down.

Suppose that

$$0 < \lambda_1 < \cdots \le \lambda_k < \lambda = f'(0) < \lambda_{k+1} \le \cdots \to \infty\,.$$

By integrating by parts, it is easy to see that the Hessian of J at the trivial solution $h = D^2J(0)$ can be represented by the diagonal matrix with entries

$$h_{ii} = \lambda_i - \lambda\,.$$

Therefore $\mathrm{sig}(D^2J(0)) = k$ and it follows that the trivial solution has MI k, where k is the number of eigenvalues of $-\Delta$ less than $\lambda = f'(0)$.

Our original idea was to form a new search direction (or projected gradient) by simply changing the sign of the components of $\nabla J(u)$ lying in the negative space of D^2J. A similar and better idea is to use Newton's method acting on the gradient [see Eq. (12)]. The Newton search direction is

$$(D^2J(u))^{-1}\nabla J(u) = \sum_{i=1}^{\infty} \frac{1}{\beta_i}\langle \nabla J(u),\, e_i\rangle e_i\,,$$

where (β_i, e_i) are the orthonormal eigenpairs of $D^2J(u)$, that have been used to construct $(D^2J(u))^{-1}$. Note that when $\text{sign}(\beta_i) < 0$, the component of $\nabla J(u)$ along the "concave down" e_i direction is reflected as well as scaled, so that in effect Newton's method automatically performs weighted ascent in this direction. In "concave up" directions e_i where $\text{sign}(\beta_i) > 0$, the sign remains the same and the search direction is weighted descent. In this way, Newton's method on the gradient seeks minimax critical points of arbitrary MI depending on the signature of u. We see this as a generalization of the method for finding MI 1 and MI 2 minimax solutions described in [Neuberger, 1997a, 1997b].

As a practical matter, since $D^2J(u)$ may be noninvertible or ill conditioned, one should consider using singular value decomposition and pseudoinverses, least squares, or a system solver which handles our possible types of singularities when computing this search direction. For nondegenerate solutions, the Hessian is nonsingular in a neighborhood of the solution and the pseudoinverse is not needed. However, we are sometimes interested in degenerate solutions, for example at bifurcation points or nonradial solutions to the PDE on a disk where there is a continuum of solutions. We have found the algorithm to be surprisingly robust even when an actual inverse is computed and used very near a singularity, an interesting phenomena worthwhile for future study. In several examples the corresponding zero-eigenfunction directions were nearly orthogonal to nearby gradients, and hence had little effect on the projected gradient search direction.

It is well known that Newton's method converges very well given a good initial guess and is unpredictable given a poor initial guess. Our experiments confirm this. We were able to obtain a methodology for generally providing an initial guess that would lead to convergence to a predicted and desired solution, i.e. start and remain in the correct basin of attraction. Our rule of thumb is to use an appropriate multiple of an eigenfunction having a prescribed nodal structure and signature. When f is odd, this works well provided the multiple is in the right ball park; we can use the observation that $\lim_{\alpha\to\infty} \text{sig}(\alpha\psi_i) = \infty$ for all $i \in \mathbf{N}$ to obtain the appropriate multiplier. When f is not so nice, solutions may have nodal structures that do not closely match that of eigenfunctions, whereby multiples of eigenfunctions may not be good starting points. In this case it can be necessary to look for solutions by first starting near primary bifurcation points which do closely resemble eigenfunctions. One then increments or decrements the bifurcation parameter to follow the branch towards the desired solution, at each step using the previous solution as the next initial guess. The matter is somewhat more delicate at secondary bifurcation points. In this case we add a small linear combination of zero-eigenfunctions of $D^2J(u)$ to a nearby element of the primary branch, where u is the singular bifurcation point. The same philosophy applies for finding tertiary branches off of secondary branches.

To apply Newton's method to our problem, we truncate the infinite dimensional function space H to the finite dimensional Galerkin space $G = \text{span}\{\psi_i\}_{i=1}^M$. We restrict all of our computations to the M-dimensional subspace $G \subset H$. Recall that we have normalized our eigenfunctions in L_2 so that $\int_\Omega \psi_i\psi_j dx = \delta_{ij}$ and $\int_\Omega \nabla\psi_i\nabla\psi_j dx = \delta_{ij}\lambda_i$, where δ_{ij} is the Kronecker delta function.

Thus, we identify G with $\mathbf{R}^M$ and define $\hat{J} : \mathbf{R}^M \to \mathbf{R}$ by $\hat{J}(a) = J(u)$, where $u = \sum_{i=1}^M a_i\psi_i \in G$. The function $\hat{J}$ is identified with $J|_G$. Our approximate solutions to the PDE are then critical points of the function $\hat{J}$, rather than the functional J. It seems reasonable, although we have no proof, that the approximate solutions converge to the true solution as $M \to \infty$. In Sec. 5 we will consider this question of convergence, and discuss how this algorithm might inspire existence proofs.

The L_2 gradient of $\hat{J}$ is the vector function

$$g(a) = \left(\frac{\partial\hat{J}(a)}{\partial a_1}, \ldots, \frac{\partial\hat{J}(a)}{\partial a_M}\right) = (J'(u)(\psi_1), \ldots, J'(u)(\psi_M)) \in \mathbf{R}^M$$

and the Hessian matrix is

$$A(a) = \left(\frac{\partial^2\hat{J}(a)}{\partial a_i\partial a_j}\right)_{i,j=1}^M = (J''(u)(\psi_i, \psi_j))_{i,j=1}^M .$$

Using integration by parts, we see that we can compute the entries

$$g_k(a) = \frac{\partial\hat{J}(a)}{\partial a_k} = -\int_\Omega (\Delta u + f(u))\psi_k \, dx = a_k\lambda_k - \int_\Omega f(u)\psi_k \, dx \tag{13}$$

and

$$A_{jk}(a) = \delta_{jk}\lambda_j - \int_\Omega f'(u)\psi_j\psi_k \, dx , \tag{14}$$

where $u = \sum_{i=1}^{M} a_i \psi_i$. For informational purposes, one might also want to compute $\hat{J}(a) = J(u)$ in a similar fashion. Note that we only need to do numerical integration on the nonlinear terms. This greatly increases the accuracy of our approximations. With a gradient and Hessian in hand, the Newton iteration in (12) then becomes

$$a^{n+1} = a^n - (A(a^n))^{-1} g(a^n)\,.$$

In practice, one can introduce stability and remain in a desired basin of attraction by imitating a continuous Newton's flow by taking smaller steps, i.e. choose δ small and iterate

$$a^{n+1} = a^n - \delta (A(a^n))^{-1} g(a^n)\,.$$

When the sequence of coefficients $\{a^n\}$ converges to a vector a, our approximate solution is given by $u = \sum_{i=1}^{M} a_i \psi_i$. As previously noted, if this solution u is a nondegenerate critical point then computing $\mathrm{sig}(A(u))$ yields the Morse index. We find this method to be very effective and simple to implement, given that we have such ready access to the desired basis when Ω is a square. For other regions, knowing or approximating an orthonormal basis of eigenfunctions might not be so straightforward. Once such an effort was made, however, subsequent runs of the GNGA would run fast and efficiently. Sophisticated grid techniques would only be necessary in so far as they might be required by the numerical integration routines. All differencing has been eliminated by the use of the eigenfunction basis.

To summarize the GNGA for our semilinear elliptic Dirichlet problem, one performs the following steps:

1. Define region Ω, nonlinearity f, and step size δ.
2. Obtain orthonormal basis $\{\psi_k\}_{k=1}^{M}$ for a sufficiently large subspace $G \subset H$.
3. Choose initial coefficients $a = a^0 = \{a_k\}_{k=1}^{M}$, set $u = u^0 = \sum a_k \psi_k$, and set $n = 0$.
4. Loop
   (a) Calculate $g = g^{n+1} = (J'(u)(\psi_k))_{k=1}^{M} \in \mathbf{R}^M$ (gradient vector).
   (b) Calculate $A = A^{n+1} = (J''(u)(\psi_j, \psi_k))_{j,k=1}^{M}$ (Hessian matrix).
   (c) Compute $\chi = \chi^{n+1} = A^{-1} g$ by computing inverse or pseudoinverse, solving system, or implementing least squares.
   (d) Set $a = a^{n+1} = a^n - \delta\chi$ and update $u = u^{n+1} = \sum a_k \psi_k$.
   (e) Increment loop counter n.
   (f) Calculate $\mathrm{sig}(A(a))$ and $\hat{J}(a)$ if desired.
   (g) Calculate approximation $\sqrt{g \cdot g}$ of $||\nabla J(u)||$; STOP if sufficiently small.

In the following section we present an efficient method for implementing the GNGA scheme when f is polynomial. In that case, $\hat{J}$, g, and A are themselves polynomials in a, and once various integrals are calculated, no further integration need be performed. Our implementation of this polynomial GNGA was in *Mathematica* and can provide superior handling of bifurcation curves via several features not found in the nonpolynomial FORTRAN code.

3.2. *The algorithm for polynomial f*

When the reaction term f is a polynomial, the functions $\hat{J}$, g_k and $A_{j,k}$ needed for the GNGA are polynomials. The coefficients of these polynomials can be computed once and for all. Thereafter, we only need to solve Newton's method on polynomial equations, which is so fast we can do it using *Mathematica*. In contrast, for general f, many numerical integrations are performed at each step in Newton's method, and a compiled language like FORTRAN is needed.

To understand the difference between polynomial and nonpolynomial f, consider the nonlinear terms in Eqs. (13) and (14) for $g_k(a)$ and $A_{j,k}(a)$, respectively. If f is a polynomial, these nonlinear terms are polynomials in a_i, and the coefficients of the polynomial can be computed, by numerical integration if necessary, *before* doing Newton's method. On the other hand, for more complicated f this nonlinear term must be computed numerically *after* the a_i are known numbers, at each step in Newton's method.

The conditions on f described before Theorem 2.2 are called the CCN assumptions. They are quite restrictive when f is a polynomial. In fact, if the dimension of Ω is $N \geq 4$, then no polynomial satisfies the CCN assumptions. To see this, consider the first CCN assumption, and note that a polynomial f must have degree $p < N + 2/N - 2$. Hence the polynomial f must have degree strictly less than 3 for $N \geq 4$. Other assumptions rule out linear and quadratic polynomials, as described in the next paragraph.

For $N = 3$, a polynomial f satisfies the CCN assumptions if, and only if, $f(u) = \lambda u + \beta u^3$ with

$\beta > 0$. For $N = 2$, which is our focus here, it is rather cumbersome to find necessary and sufficient conditions that the polynomial f satisfy the CCN assumptions. One necessary condition is that $f''(0) = 0$, which follows from $f'(u) \geq f(u)/u$ for all $u \neq 0$. Hence there is no quadratic term in the polynomial f. Another necessary condition is that f must have odd degree at least 3, with positive leading coefficient, since $f(u)/u \to \infty$ as $|u| \to \infty$. Heuristically, the CCN assumptions say that "f is very much like an odd function."

Therefore, if f is a nonodd polynomial that satisfies the CCN assumptions for dimension $N = 2$ it must have degree at least 5. Our algorithm is too slow to run on *Mathematica* when f is a polynomial of degree 5, so we assume that f is cubic, with a positive leading coefficient that has been scaled to unity:

$$f(u) = \lambda u + \alpha u^2 + u^3 \,. \tag{15}$$

The polynomial (15) satisfies the CCN assumptions if, and only if, $\alpha = 0$. However, we will consider the effects of nonzero α. This makes f nonodd in a more radical way than allowed by the CCN assumptions. One interesting result we find is that, when $\alpha \neq 0$, certain solutions bifurcate transcritically from the trivial solution. In other words, there are small amplitude solutions near $\lambda = \lambda_i$ for both $\lambda > \lambda_i$ and $\lambda < \lambda_i$. In contrast, the CCN assumptions force the small amplitude solutions to bifurcate to $\lambda < \lambda_i$.

Assume that the reaction term is (15), with the parameters λ and α fixed. The action functional on the domain H,

$$J(u) = \int_\Omega \left(\frac{|\nabla u|^2}{2} - \frac{\lambda u^2}{2} - \frac{\alpha u^3}{3} - \frac{u^4}{4} \right) dx \,,$$

is then approximated by a polynomial in the amplitudes of the Galerkin expansion:

$$\hat{J}(a) = \frac{1}{2} \sum_{p=1}^{M} (\lambda_p - \lambda) a_p^2 - \frac{\alpha}{3} \sum_{p,q,r=1}^{M} a_p a_q a_r I_{pqr} - \frac{1}{4} \sum_{p,q,r,s=1}^{M} a_p a_q a_r a_s I_{pqrs} \,. \tag{16}$$

We have defined the integral of the product of two or three eigenfunctions as

$$I_{pqr} = \int_\Omega \psi_p \psi_q \psi_r dx, \quad \text{and} \quad I_{pqrs} = \int_\Omega \psi_p \psi_q \psi_r \psi_s dx \,.$$

The critical points of $\hat{J}$ are our approximate solutions to the PDE. They are solutions to the M equations

$$g_i(a) = \frac{\partial \hat{J}(a)}{\partial a_i} = (\lambda_i - \lambda) a_i - \alpha \sum_{p,q=1}^{M} a_p a_q I_{ipq} - \sum_{p,q,r=1}^{M} a_p a_q a_r I_{ipqr} = 0 \,.$$

Finally, the Hessian operator is approximated by the Hessian matrix

$$A_{ij}(a) = \frac{\partial^2 \hat{J}(a)}{\partial a_j \partial a_i} = (\lambda_i - \lambda)\delta_{ij} - 2\alpha \sum_{p=1}^{M} a_p I_{ijp} - 3 \sum_{p,q=1}^{M} a_p a_q I_{ijpq} \,.$$

To speed up the calculations, we supply the Hessian to *Mathematica's* built-in FindRoot command as the Jacobian of the system of equations: $A_{ij} = \partial g_i / \partial a_j$. The Hessian matrix is also needed to compute the MI of the solutions.

The multiple sums have quite a few terms. In practice, we can take advantage of the permutation symmetry of the terms in the sum. Consider the last sum in (16). Define $A_{pqrs} = a_p a_q a_r a_s I_{pqrs}$, and note that this expression is invariant under all 24 permutations of the subscripts. We can speed up the sum by an asymptotic factor of 24 (for large M) by summing only over terms with $p \geq q \geq r \geq s$, including multinomial coefficients:

$$\sum_{p,q,r,s} A_{pqrs} = \sum_p A_{pppp} + \sum_{p>q} (4A_{pppq} + 4A_{pqqq} + 6A_{ppqq}) + 12 \sum_{p>q>r} (A_{ppqr} + A_{pqqr} + A_{pqrr}) + 24 \sum_{p>q>r>s} A_{pqrs} \,.$$

The factor of $12 = 4!/(2! \cdot 1! \cdot 1!)$ comes from the partition $4 = 2 + 1 + 1$. The other multinomial coefficients can be computed just as easily.

The other sums can also be written more efficiently: Assume that B_{pqr} is unchanged under all six permutations of the indices, and that $C_{pq} = C_{qp}$. Then

$$\sum_{p,q,r} B_{pqr} = \sum_p B_{ppp} + 3 \sum_{p>q} (B_{ppq} + B_{pqq}) + 6 \sum_{p>q>r} B_{pqr} \,,$$

and

$$\sum_{p,q} C_{pq} = \sum_{p} C_{pp} + 2\sum_{p>q} C_{pq}\,.$$

For any region Ω, the eigenfunctions and eigenvalues could be computed (perhaps numerically), and then all the integrals I_{pqr} and I_{pqrs} could be computed and stored in a table, rather than computing several integrals at each step in Newton's method.

We now specialize to the problem of a square region, where we can use *formulas* for the integrals I_{pqr} and I_{pqrs}. Let $\Omega = (0,\,1)\times(0,\,1)$. The normalized eigenfunctions of $-\Delta$ that we used in our Galerkin expansion are $\psi_i = \psi_{m_i,n_i}$, given in Eq. (2), where (m_i, n_i) take on all ordered pairs in $\{1,\,2,\ldots,\,N_{\max}\}^2$ as i goes from 1 to $M = N_{\max}^2$. Therefore, we have two ways of expressing the Galerkin expansion:

$$u(x,\,y) = \sum_{i=1}^{M} a_i\psi_i(x,\,y) = \sum_{m=1}^{N_{\max}}\sum_{n=1}^{N_{\max}} a_{m,n}\psi_{m,n}(x,\,y).$$

In the *Mathematica* implementation we used $N_{\max} = 3$, 5, and 7, whereas with the FORTRAN program we could go up to $N_{\max} = 15$ with a reasonable run time.

In anticipation of computing the integrals of eigenfunctions, let us define $s3(p,\,q,\,r)$ and $s4(p,\,q,\,r,\,s)$ for integers p, q, r and s as the one-dimensional integrals of products of sine functions:

$$s3(p,\,q,\,r) = \int_0^1 \sin(p\pi x)\sin(q\pi x)\sin(r\pi x)dx$$

$$s4(p,\,q,\,r,\,s) = \int_0^1 \sin(p\pi x)\sin(q\pi x)\sin(r\pi x)\cdot\sin(s\pi x)dx\,.$$

These integrals can be computed easily using Euler's formula to write the sines in terms of complex exponentials. The results are

$$s3(p,\,q,\,r) = \begin{cases} 0 \;\text{ if }\; p+q+r \;\text{ is even} \\ \dfrac{1}{2\pi}\left(\dfrac{-1}{p+q+r} + \dfrac{1}{-p+q+r} + \dfrac{1}{p-q+r} + \dfrac{1}{p+q-r}\right) \;\text{ if }\; p+q+r \;\text{ is odd} \end{cases}$$

and

$$s4(p,\,q,\,r,\,s) = \frac{1}{8}\begin{pmatrix} \delta_{p+q,r+s} + \delta_{p+r,q+s} + \delta_{p+s,q+r} - \delta_{p,q+r+s} \\ -\delta_{q,p+r+s} - \delta_{r,p+q+s} - \delta_{s,p+q+r} \end{pmatrix}.$$

Then the integrals of eigenfunctions are

$$I_{pqr} = 8s3(m_p,\,m_q,\,m_r)s3(n_p,\,n_q,\,n_r)$$

and

$$I_{pqrs} = 16s4(m_p,\,m_q,\,m_r,\,m_s)s4(n_p,\,n_q,\,n_r,\,n_s)\,.$$

Now all the ingredients are in place to find approximate solutions to our PDE. We used the "FindRoot" command in *Mathematica*, which uses Newton's method, to solve the system of M polynomial equations $g_i(a;\,\lambda,\,\alpha) = 0$. Usually we fixed the parameters λ and α in (15), and let the amplitudes a be the M unknowns. Sometimes we fixed α and a single amplitude, and used λ and the rest of the amplitudes as the M unknowns. Yet another method was to fix α and the ratio of two amplitudes. Then one amplitude can be eliminated, and the unknowns are λ and the other $M-1$ amplitudes.

4. Numerical Results on the Square

In this section we display results of our Newton–Galerkin method for the BVP (1) on the square $\Omega = (0,\,1)\times(0,\,1)$. We usually use $f(u) = \lambda u + u^3$, and consider λ to be a bifurcation parameter. We also consider more general f, and give a classification of the types of bifurcation from the trivial solution that are to be expected for different classes of the function f, depending on the symmetry of the critical eigenfunction(s) at the bifurcation.

Since the square has symmetry, we use the methods of bifurcation theory with symmetry [Golubitsky *et al.*, 1988]. Care is needed to analyze the bifurcation correctly. In particular, our problem exhibits a "hidden" translational symmetry when f is odd [Crawford *et al.*, 1991; Gomes *et al.*, 1999]. This hidden symmetry can force patterns whose symmetries are different subgroups of the symmetry of the square to have identical solution curves when the norm of the solution is plotted against λ.

4.1. *The symmetry of the PDE on the square*

Let $\mathbf{D}_4$ be the symmetry of the square $\Omega = (0, 1) \times (0, 1)$. Note that $\mathbf{D}_4$ is generated by two involutions μ and δ, which act on the square as follows:

$$\mu \cdot (x, y) = (1 - x, y) \quad \text{and} \quad \delta \cdot (x, y) = (y, x) .$$

We define $\rho = \mu\delta$, which acts as a 90° rotation. Furthermore, we define $\tilde{\mu} = \rho^{-1}\mu\rho$ and $\tilde{\delta} = \rho^{-1}\delta\rho$. Thus, μ and $\tilde{\mu}$ act as mirror reflections across $x = 1/2$ and $y = 1/2$, respectively, whereas δ and $\tilde{\delta}$ act as reflections across the diagonals.

The group $\mathbf{D}_4$ acts on functions in H as well: $\mu \cdot u(x, y) = u(1 - x, y)$ and $\delta \cdot u(x, y) = u(y, x)$. If $u(x, y)$ is a solution to the PDE, then so is $\gamma \cdot u(x, y)$, for any $\gamma \in \mathbf{D}_4$. Sometimes γ takes one solution to a different solution, but if $\gamma \cdot u = u$ we say that γ is a symmetry of the solution u. We define the symmetry group of a function $u \in H$ to be

$$\Sigma(u) = \{\gamma \in \mathbf{D}_4 : \gamma \cdot u = u\} .$$

For functions in the Galerkin space G, the symmetry group acts as

$$\begin{aligned} \mu \cdot u(x, y) &= u(1 - x, y) \\ &= \sum_{m=1}^{N_{\max}} \sum_{n=1}^{N_{\max}} (-1)^{m+1} a_{m,n} \psi_{m,n}(x, y) \end{aligned}$$

and

$$\delta \cdot u(x, y) = u(y, x) = \sum_{m=1}^{N_{\max}} \sum_{n=1}^{N_{\max}} a_{n,m} \psi_{m,n}(x, y) .$$

Thus, the $\mathbf{D}_4$ action on the space of amplitudes is generated by

$$\mu \cdot a_{m,n} = (-1)^{m+1} a_{m,n} \quad \text{and} \quad \delta \cdot a_{m,n} = a_{n,m}$$

When f is odd, i.e. $f(-u) = -f(u)$, the symmetry group of the PDE is $\mathbf{D}_4 \times \mathbf{Z}_2$, where the $\mathbf{Z}_2$ action on functions in H is

$$\sigma \cdot u(x, y) = -u(x, y) .$$

This induces the $\mathbf{Z}_2$ action on the amplitudes: $\sigma \cdot a_{m,n} = -a_{m,n}$.

4.2. *The consequences of odd f*

Clearly, if f is odd and $u(x, y)$ is a solution to $\Delta u + f(u) = 0$, then $-u(x, y)$ is also a solution. It is known that there are an infinite number of solutions to the superlinear problem on any region when f is odd [Ljusternik & Schnirelmann, 1934]. However, only three solutions have been proven to exist for general f in a general region of dimension $N \geq 2$, see [Castro & Kurepa, 1987; Castro *et al.*, 1997; Tehrani, 1996; Wang, 1991].

To explore the effects of f being odd, we will temporarily consider solutions of (1) on the rectangle. We will then tile the plane with copies of the solution reflected to make a "checkerboard" pattern. This will be used for two purposes: First, to show that an infinite number of solutions on the square exist when f is odd. Second, to show that there can be a "hidden" translational symmetry between patterns on the square that look quite different.

Suppose $u_{a,b}(x, y)$ is a solution to (1) on the rectangle $\bar{\Omega} = [0, a] \times [0, b]$ with zero Dirichlet boundary conditions, and f is odd. Then we define the tiled solution $u^t_{a,b}(x, y)$ obtained by reflection across the boundaries:

$$\begin{aligned} u^t_{a,b}(2a - x, y) &= -u^t_{a,b}(x, y) \\ \text{and} \qquad u^t_{a,b}(x, 2b - y) &= -u^t_{a,b}(x, y) \end{aligned} \tag{17}$$

It can be shown that u^t is a solution to the PDE (1) on $\Omega = \mathbf{R}^2$ if f is odd. In place of the boundary conditions in (1), $u^t_{a,b}(x, y)$ satisfies periodic boundary conditions: u^t is $2a$-periodic in the x direction and $2b$-periodic in the y direction.

Now there is a simple constructive proof that there are an infinite number of solutions to the superlinear problem on the square when f is odd. (The LS theory [Ljusternik & Schnirelmann, 1934] for general regions is quite complicated.) For any pair of positive integers m and n, it is well known

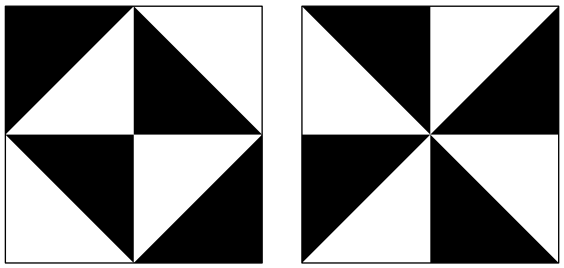

(a) (b)

Fig. 1. Two solutions of the BVP (1), with f odd, related by a "hidden" translational symmetry. The white indicates $u > 0$, and the black indicates $u < 0$, in this and the following figures. When the two patterns are tiled (periodically extended by reflection across the boundaries) they are the same except for a vertical translation of half a unit.

that there is a positive solution to (1) on the rectangle $[0,\, 1/m] \times [0,\, 1/n]$. Let $u_{1/m,1/n}(x,\, y)$ be this positive solution, then the corresponding tiled solution $u^t_{1/m,1/n}(x,\, y)$ is a solution to (1) on the unit square. Note that these tiled solutions are very much like the eigenfunctions $\psi_{m,n}$.

The hidden translational symmetry of a solution occurs if a solution, when tiled, can be translated to fit on the square in a different way. For example, Fig. 1(a) shows a solution $u_{1,1}(x,\, y)$ with hidden translational symmetry. Figure 1(b) shows the tiled and translated solution $u^t_{1,1}(x,\, y-1/2)$, restricted to the unit square. The two solutions have exactly the same action $J(u)$, the same L_2 norm $\|u\|_2$, and the same supremum norm $\|u\|_\infty$.

There is a different way to understand the hidden translational symmetry: Note that the solutions shown in Fig. 1 can be obtained by tiling two different solutions on $[0,\, 1/2] \times [0,\, 1/2]$ (the lower left corner). These sign-changing exactly once solutions (CCN solutions) are proved to exist on the smaller square by Theorem 2.2. On the smaller square, the two solutions are related by a rotation. However, when they are tiled to the unit square, the resulting solutions are not related by any symmetry of the square.

4.3. *Bifurcations from the trivial solution*

With our assumption that $f(0) = 0$, $u = 0$ is always a solution, which we call the trivial solution, or the origin. The MI of the trivial solution is the number of eigenvalues of $-\Delta$ smaller than $f'(0)$. (The MI is undefined if $f'(0)$ is equal to any of the eigenvalues.) We take $f'(0) = \lambda$ to be the bifurcation parameter. Whenever λ passes through one of the eigenvalues of the negative Laplacian there is a bifurcation of solutions from the origin.

The type of bifurcation that occurs depends on many factors: the multiplicity of the eigenvalue, the parity of the eigenfunctions, and the details of the function f. We will concentrate on bifurcations at eigenvalues with multiplicity 1 or 2. We will give the form of the Liapunov–Schmidt bifurcation equations for the single amplitude

$$a = a_{m,m}$$

in the multiplicity 1 case, or the pair of amplitudes

$$a = a_{m,n} \quad \text{and} \quad b = a_{n,m}$$

in the case with multiplicity 2. We are assuming that there are no degeneracies that lead to higher multiplicity. The first two such degeneracies are $\lambda_{1,7} = \lambda_{5,5} = 50\pi^2$ which lead to an eigenvalue of $-\Delta$ with multiplicity 3, and $\lambda_{1,8} = \lambda_{4,7} = 65\pi^2$ which leads to an eigenvalue of multiplicity 4.

It is convenient to express the results of the Liapunov–Schmidt reduction in terms of a reduced action functional: $\tilde{J} = p(a,\, \lambda)$ or $\tilde{J} = p(a,\, b,\, \lambda)$. In the multiplicity 2 case, the function p is symmetric under interchange of the first two arguments; that is $p(a,\, b,\, \lambda) = p(b,\, a,\, \lambda)$. The Liapunov–Schmidt reduced equations for the elliptic PDE (1) take the form

$$\frac{\partial \tilde{J}}{\partial a} = 0, \quad \frac{\partial \tilde{J}}{\partial b} = 0$$

whereas the center manifold reduction of the hyperbolic PDE (7) takes the form

$$\dot{a} = \frac{\partial \tilde{J}}{\partial a}, \quad \dot{b} = \frac{\partial \tilde{J}}{\partial b}\,.$$

In the multiplicity 1 case, of course, only the first equation (with the derivative with respect to a) is needed.

In the case when f is odd, we are indebted to the work of Gomes and Stewart [1994]. They studied bifurcations with Neumann boundary condition. Their results can be applied to our problem, with Dirichlet boundary conditions, if and only if f is odd in our problem. The first step is to factor out the greatest common divisor of m and n, $r = \gcd(m,\, n)$. Thus

$$(m,\, n) = r(k,\, \ell)\,. \tag{18}$$

The physical meaning of this reduction is that the pattern on the little square $[1,\, 1/r] \times [1,\, 1/r]$ is extended in a checkerboard pattern so that r^2 tiles fill the unit square.

Note that if $m = n$, then $k = \ell = 1$. Gomes and Stewart [1994] prove that the normal form depends on whether k and ℓ have the same or opposite parity. They cannot both be even, since k and ℓ are relatively prime.

The table entries for the case where f is not odd follow simply from considering the action of the two reflections μ and δ on the amplitudes a and b. If m is odd and n is even then $\mu(a,\, b) = (a,\, -b)$. If m and n are both even then $\mu(a,\, b) = (-a,\, -b)$. If m and n are both odd then $\mu(a,\, b) = (a,\, b)$. On the other hand, the action of the diagonal reflection does not depend on the parity of m or n: $\delta(a,\, b) = (b,\, a)$.

The following table summarizes the effects of symmetry on the reduced action function $\tilde{J}$ for λ in the neighborhood of $\lambda_{m,n}$: See Eq. (18) for the meaning of k and ℓ in the case where f is odd.

f odd	$m = n$	$\tilde{J} = p(a^2,\, \lambda)$
	$k \neq \ell,$ even/odd	$\tilde{J} = p(a^2,\, b^2,\, \lambda)$
	$k \neq \ell,$ odd/odd	$\tilde{J} = p(a^2,\, b^2,\, (ab)^{\max(k,\,\ell)},\, \lambda)$
f not odd	$m = n,$ even	$\tilde{J} = p(a^2,\, \lambda)$
	$m = n,$ odd	$\tilde{J} = p(a,\, \lambda)$
	$m \neq n,$ odd/even	$\tilde{J} = p(a^2,\, b^2,\, \lambda)$
	$m \neq n,$ even/even	$\tilde{J} = p(a^2,\, b^2,\, ab,\, \lambda)$
	$m \neq n,$ odd/odd	$\tilde{J} = p(a,\, b,\, \lambda)$

(19)

Figure 2 shows the small-amplitude solutions created at bifurcations that are representative of all bifurcations from the origin with multiplicity 1 or 2. Only one representative of each group orbit of solutions is shown. The group is $\mathbf{D}_4 \times \mathbf{Z}_2$ or $\mathbf{D}_4$, depending on if f is odd or not. The size of the group orbit is indicated by the small number. When f is odd, the symmetry group is $\mathbf{D}_4 \times \mathbf{Z}_2$, and the positive and negative solutions are related by the symmetry $\sigma \in \mathbf{Z}_2$, since $\sigma \cdot u = -u$. On the other hand, when f is not odd and the symmetry group is $\mathbf{D}_4$, the positive and negative solutions are either distinct (if m and n are both odd) or related by a symmetry of the square (if m or n is even).

The upper row of solutions in each case of Fig. 2 has $f(u) = \lambda u + u^3$, and the solutions are some multiples of the eigenfunctions shown, plus harmonics. The solutions below these are obtained with $f(u) = \lambda u + 2u^2 + u^3$. (We set λ to be π^2 below the bifurcation value.)

Figure 2 is divided based on the cases when f is not odd in Table 19. When f is odd, one must first do the reduction $(m,\, n) = r(k,\, \ell)$ and then find the appropriate entry in Table 19. For example, $(m,\, n) = (2,\, 4) = 2(1,\, 2)$ is shown in Fig. 2. When f is odd, the normal form for the $(2, 4)$ case is the same as the $(1, 2)$ case. Note how the lower-left corner of the $(2,\, 4)$ solutions are the same as the whole square in the $(1, 2)$ case, when f is odd. The two mixed-mode solutions in the $(2, 4)$ case are related by a hidden translational symmetry, as shown in Fig. 1, but they are in different $\mathbf{D}_4 \times \mathbf{Z}_2$ group orbits.

The case where $m = n$ and both are odd deserves special attention because it is the most "generic" case. For general regions the eigenvalues of the Laplacian typically have multiplicity 1, and there are no reflections of the region that take an eigenfunction into its negative. For this reason, we have explored the bifurcation at $(m,\, n) = (1,\, 1)$ in greater depth, focusing on the effects caused by different types of functions f. The results are shown in Fig. 3.

When f is odd, there is a pitchfork bifurcation as shown in the first row of Fig. 3, where $f(u) = \lambda u + u^3$.

When f is not odd, the plus and minus branches are no longer related by the symmetry $u \to -u$. However, if f is C^2 and $f''(0) \neq 0$, then f does not satisfy condition (10). In the middle row of

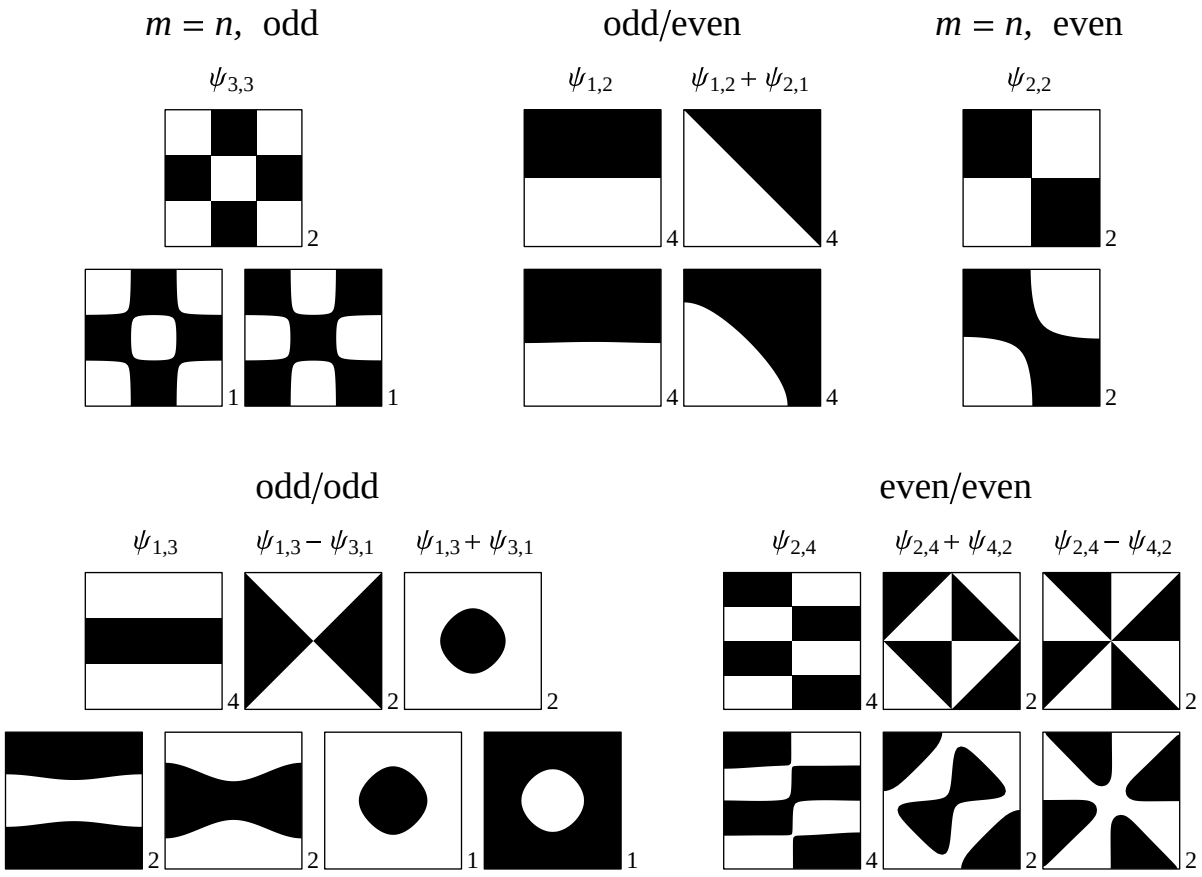

Fig. 2. The solution types which bifurcate at $\lambda = \lambda_{m,n} = (m^2 + n^2)\pi^2$. The five cases shown are based on the classification in Table 19 when f is not odd. Solutions for f odd are shown above solutions obtained with f not odd. The eigenfunctions listed correspond to the small-amplitude solutions when f is odd. Only one solution in each group orbit is shown; the number indicates the size of the group orbit. The CCN solution for the square is the one whose eigenfunction structure is $\psi_{1,2} + \psi_{2,1}$.

Fig. 3, we consider the bifurcation diagram with $f(u) = \lambda u + u^3$ if $u \geq 0$ and $f(u) = \lambda u + u^5$ if $u < 0$, which does satisfy all the conditions of Theorem 2.2 (the CCN conditions).

If $f''(0) \neq 0$, then the bifurcation at the origin is transcritical, as shown in the bottom row of Fig. 3, where $f(u) = \lambda u + u^2 + u^3$. This is typical of the case where f is not odd.

It is helpful to plot some $\mathbf{D}_4 \times \mathbf{Z}_2$-invariant quantity, such as $J(u)$, $\|u\|$ (the L_2 norm) or $\|u\|_\infty$ (the supremum norm), in the bifurcation diagrams. We prefer to plot $\sqrt{J(u)}$, $\|u\|^2$ or $\|u\|_\infty^2$, because the curves are asymptotic to straight lines near the bifurcation if $f(u) = \lambda u + u^3$, or more generally if f is odd, $f \in C^3$, and $f'''(0) \neq 0$. This asymptotic linearity can be proved for the bifurcation from a simple eigenvalue [Rabinowitz, 1986] using a Liapunov–Schmidt reduction of the bifurcation equations. Our numerical results in Fig. 3 indicate a very slight deviation from a straight line in the bifurcation diagram of the positive branch when $f(u) = \lambda u + u^3$ (upper row) and $\|u\|_\infty^2$ is plotted as against λ (right column).

Now we focus on the bifurcation diagram for $f(u) = \lambda u + u^3$, and consider the branches that bifurcate from the origin at $\lambda \leq \lambda_{2,3} = 13\pi^2$. This does not include any of the eigenvalues with multiplicity 3 or more, so Table 19 is sufficient. These branches are shown in Fig. 4.

Observe in the figure that one, two, or three curves bifurcate from the origin when λ is an eigenvalue of $-\Delta$. The next few paragraphs will explain this.

At a bifurcation from a simple eigenvalue ($m = n$), there is a pitchfork bifurcation that creates two solutions with the same action J. Hence one branch is observed bifurcating from $2\pi^2$ and $8\pi^2$ in Fig. 4. For the superlinear problem it is well known [Rabinowitz, 1986] that the nontrivial branch exists for $\lambda < \lambda_{m,m}$, as indicated in the figure.

According to Table 19, the double eigenvalues lead to two types of bifurcation. If k or ℓ is

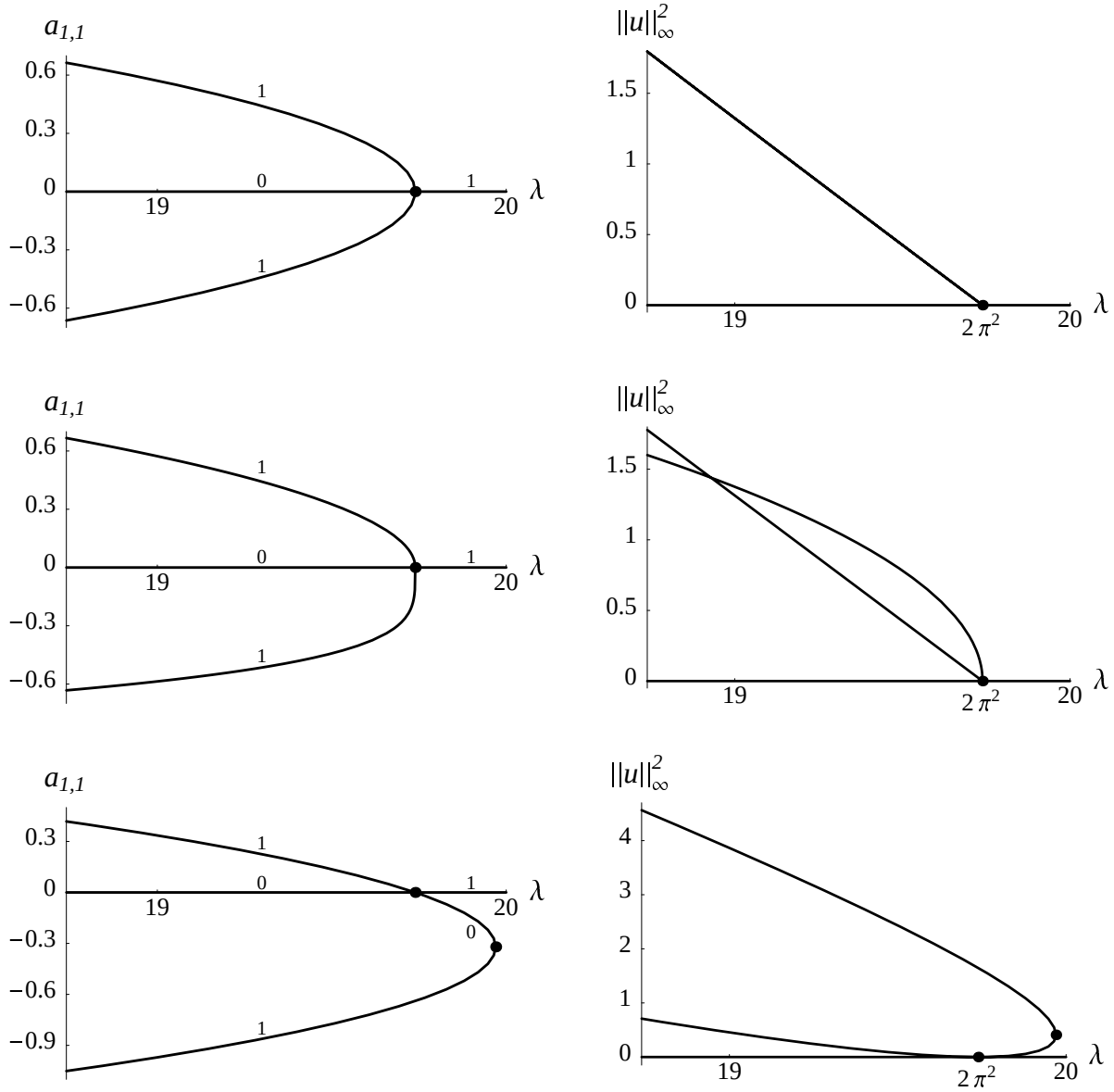

Fig. 3. Bifurcation from the origin at $\lambda = \lambda_{1,1} = 2\pi^2$. In each row the same f is used, but two different functions of u are plotted, as indicated. The first row is obtained with an odd f. In the second row, f is not odd, but $f''(0) = 0$. The third row has a nonodd f with $f''(0) \neq 0$. The Morse Index of each solution is either 0 or 1, as indicated in the figure on the left.

even (where $(m, n) = r(k, \ell)$, and $\gcd(k, \ell) = 1$) then there are two types of solutions that bifurcate: *pure modes* and *mixed modes*. Near the bifurcation, the pure modes are asymptotically a multiple of an eigenfunction $\pm\psi_{m,n}$ or $\pm\psi_{n,m}$, defined in Eq. (2). The mixed modes are asymptotic to a multiple of one of the four combinations of eigenfunctions $\pm\psi_{m,n} \pm \psi_{n,m}$. (Note that these linear combinations are themselves eigenfunctions of $-\Delta$.) When $\|u\|$ or $J(u)$ is plotted against λ, all four pure modes make one branch, and all four mixed modes make another branch. This is what we observe for $(m, n) = (1, 2)$ and $(2, 3)$ in Fig. 4. The bifurcation in this case is a standard stationary bifurcation with $\mathbf{D}_4$ symmetry. See [Golubitsky *et al.*, 1988].

On the other hand if k and ℓ are both odd, as in $(m, n) = (k, \ell) = (1, 3)$, then the bifurcation is more exotic. The mixed-mode solutions separate into two types: The *plus* solutions are asymptotically a multiple of $\psi_{m,n} + \psi_{n,m}$, and the *minus* solutions are asymptotically a multiple of $\psi_{m,n} - \psi_{n,m}$. The plus and minus solutions are separated due to the terms involving $(ab)^{\max(k,\ell)}$ in Table 19. Hence there are three branches bifurcating from $\lambda_{1,3}$ in Fig. 4.

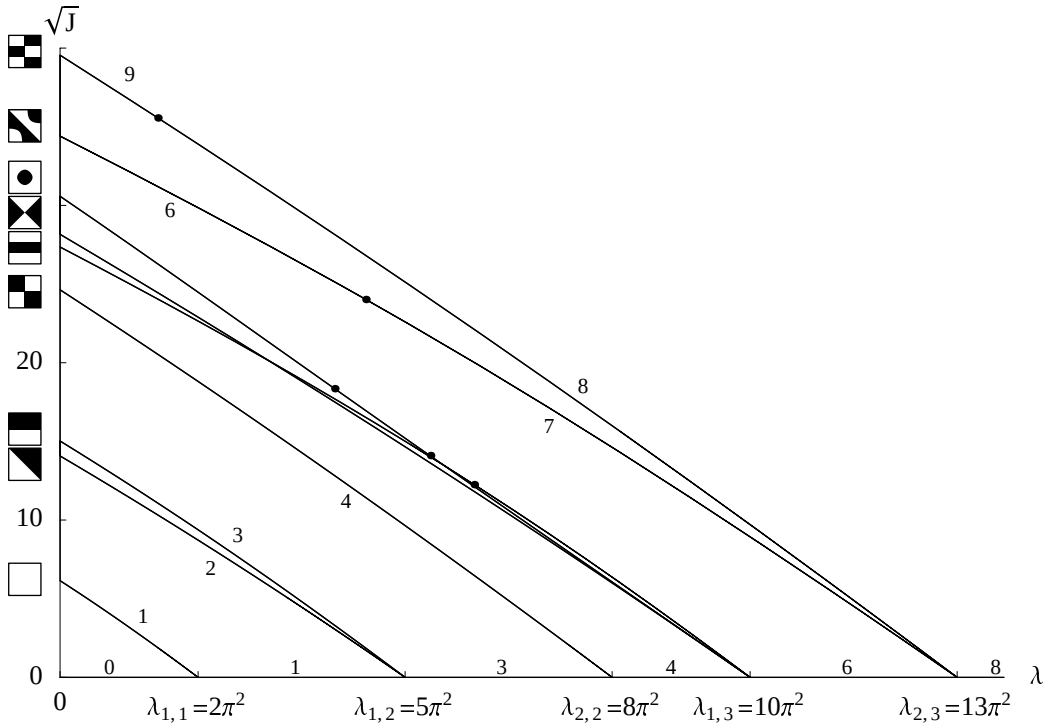

Fig. 4. Bifurcation diagram showing $\sqrt{J}$ as a function of λ, for $f(u) = \lambda u + u^3$. Only the primary branches (the ones which bifurcate from the origin) are shown. The MI is indicated by the small numbers. The dots indicate where the MI changes at secondary bifurcations which create solutions that are not shown in this figure. More details of the three branches that bifurcate from $\lambda_{1,3}$ are given in the following two figures.

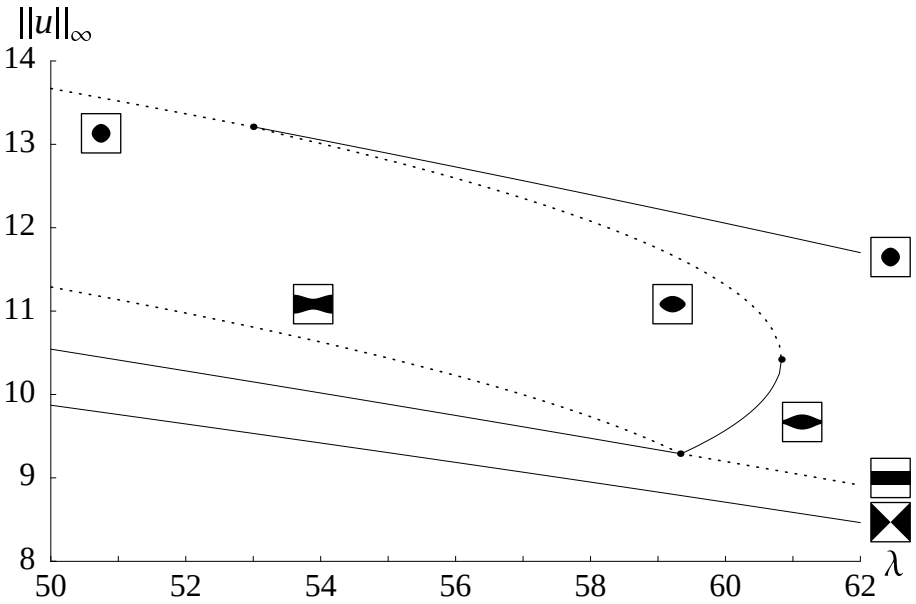

Fig. 5. Details of Fig. 4 for the branches that bifurcate from $\lambda_{1,3}$. The supremum norm, $\|u\|_\infty$, is plotted against λ because it gives a good separation between the branches. The solutions with MI 5 are solid lines, and the solutions with MI 6 are dotted lines. This figure was computed with $N_{\max} = 9$ (81 modes).

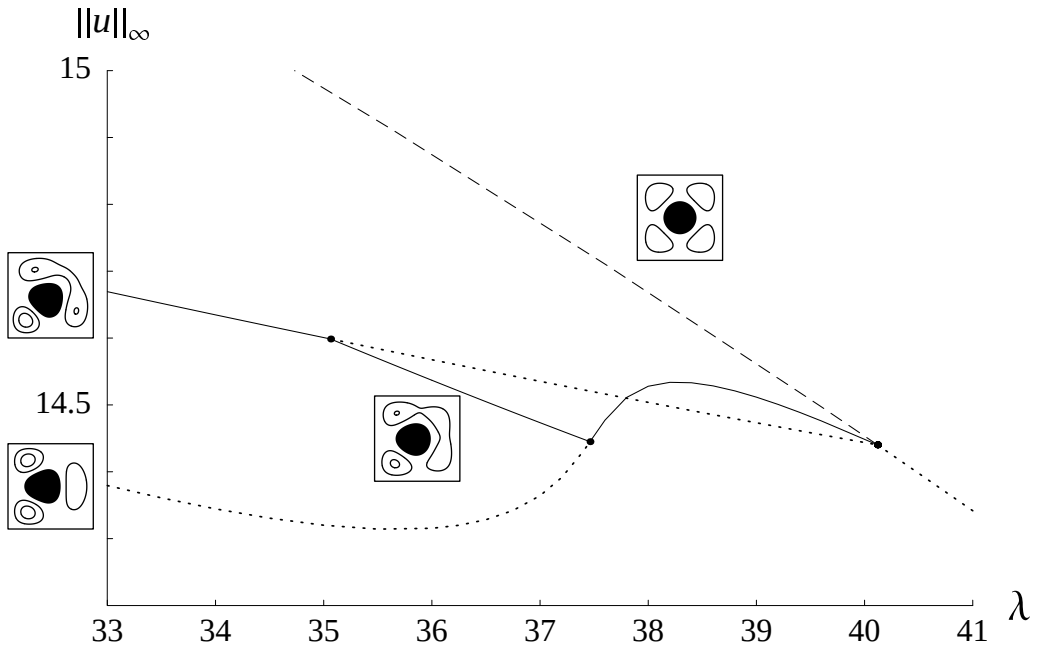

Fig. 6. Further details of Fig. 4. The plus solution undergoes a bifurcation with $\mathbf{D}_4$ symmetry at $\lambda \approx 40$, creating the vertex and edge solutions. These secondary solutions in turn bifurcate, creating a branch of tertiary solutions that exist for λ in the approximate interval $[35.1, 37.5]$. These tertiary solutions have no symmetry. The Morse indices are indicated by the line type: MI 6 are dotted, MI 7 are solid and MI 8 are dashed lines. Along with the black region, showing where $u < 0$, the contours at $u = 1/3\|u\|_\infty$ and $u = 2/3\|u\|_\infty$ are shown to better see the symmetry of the patterns. This figure was computed with $N_{\max} = 7$ (49 modes).

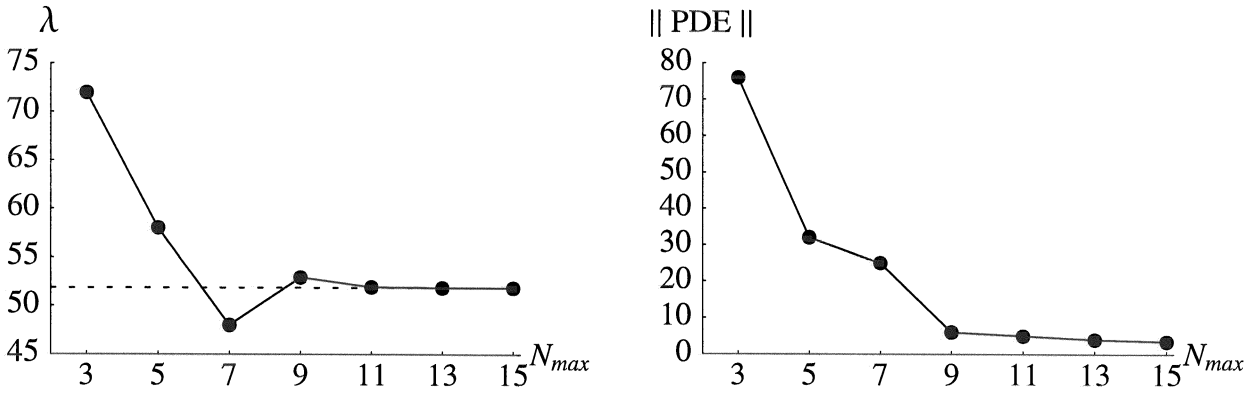

(a) (b)

Fig. 7. Convergence as the number of modes, $M = N_{\max}^2$, increases. (a) shows the λ value of the secondary bifurcation of the plus solution seen in Fig. 5, as a function of $N_{\max}$. (b) shows the L_2 norm of the PDE, $\|\Delta u + u^3\|_2$, as a function of $N_{\max}$, for the CCN solution. (The CCN solution on the square is asymptotically proportional to $\psi_{1,2} + \psi_{2,1}$ at small amplitude.)

The solutions which bifurcate from $\lambda_{1,3}$ are the most interesting, and we have studied them further. Near the primary bifurcation, the pure mode has MI 6 and a larger J (or $\|u\|$) than the plus and minus solutions, which have MI 5 and approximately the same J. These primary solutions undergo secondary bifurcations at λ approximately 59, 53, and 40, as described in the next two figures.

Figure 5 shows the two secondary bifurcations for larger λ values. In addition to the three primary branches (plus, minus, and pure mode), Fig. 5 shows a secondary solution branch with solutions of the form $a\psi_{1,3} + b\psi_{3,1}$ with a and b nonzero and $a^2 \neq b^2$. We call these solutions *rectangles* because they have the symmetry of a rectangle. The rectangle branch starts at a pitchfork bifurcation of the

plus solution at $\lambda \approx 53$ that creates rectangles with $ab > 0$. The rectangle branch has a saddle-node bifurcation at $\lambda \approx 61$, then takes part in a transcritical bifurcation of the pure mode solution at $\lambda \approx 59$. After this transcritical bifurcation, the rectangles have $ab < 0$. This transcritical bifurcation is to be expected, because the pure mode $(a, 0)$ is forced to be a solution for $\lambda < \lambda_{1,3}$ by the hidden translational symmetry, even though the system does *not* have the symmetry $(a, b) \to (a, -b)$.

The plus solution undergoes another secondary bifurcation shown at $\lambda \approx 40$, in Fig. 6. This secondary bifurcation is a standard stationary bifurcation with $\mathbf{D}_4$ symmetry [Golubitsky *et al.*, 1988]. Eight solutions bifurcate off each plus solution: four *edge* solutions where the zero contour moves toward an edge of the square, and four *vertex* solutions, where the zero contour moves toward a vertex of the square.

It is interesting that the edge and vertex solutions themselves undergo a tertiary bifurcation that creates what we call *tertiary* solutions. These solutions have no symmetry; the eight elements of $\mathbf{D}_4$ each take the zero contour to a different set. There are eight tertiary solutions with $u > 0$ inside the zero contour and eight tertiary solutions with $u < 0$ inside the zero contour. Note the resemblance of Fig. 6 to the lower-left panel of Fig. 7.2 on p. 351 of [Golubitsky *et al.*, 1988].

Finally, we did some tests on the convergence of our results as $N_{\max}$ increases. Figure 7 shows the results. We see that the λ value of a certain bifurcation stabilizes quite nicely in Fig. 7(a). Figure 7(b) shows the L_2 norm of $\Delta u + u^3$, which should converge to 0 as $N_{\max} \to \infty$. The rather slow convergence might be due to roundoff error, or it might be due to the amplification of high-frequency modes by the Laplacian. These high-frequency modes dominate the error in an ideal implementation of our algorithm, since the algorithm attempts to find a function for which the projection of $\Delta u + u^3$ onto the Galerkin space G is zero.

5. Thoughts on Proving Existence and Convergence Theorems

In this section we discuss ideas which, if proven, may lead to existence and convergence results. Since the existence theorems we desire to prove will be of a constructive nature, we find it likely that these two types of results will share lemmas. It is thus natural to consider them both at the same time.

Our ultimate goal is to completely describe all solutions to (1), i.e. to prove the existence of all solutions and understand the nodal structure of said solutions. This is a very hard problem which has been worked on by many outstanding mathematicians. What we outline below is meant to be a suggested research direction for accomplishing that goal. We feel this approach has a fair chance of being fruitful, partly because it makes more precise the intuitively felt relationship between the eigenfunctions of $-\Delta$ and solutions of arbitrary MI and nodal complexity to (1). Of course convergence results pertaining to our numerical algorithm are related and also desirable.

We have observed that the low MI solutions are of simple nodal structure, and thus should have eigenfunction (Fourier) expansions with the first few coefficients dominating. It thus seems reasonable that for sufficiently large $M \in \mathbf{N}$, the $M \times M$ matrix $A = A(u) = (J''(u)(\psi_i, \psi_j))_{i,j=1}^M$ should approximate $D^2J(u)$ well. One can view the approximation as good in the following sense. Firstly, one should have $\mathrm{sig}(D^2J(u)) = \mathrm{sig}(A)$ and that the first few eigenvalues of $D^2J(u)$ and A closely agree. Secondly, the first few eigenvectors of A in $\mathbf{R}^M$, thought of as coordinates in the Galerkin space $G = \mathrm{span}\{\psi_i\}_{i=1}^M$, appear to closely represent the first few eigenfunctions of $D^2J(u)$ in H. If $D^2J(u)$ is invertible this seems provable. It is not clear how to handle the case where the Hessian has one or more zero-eigenvalues. Given a nondegenerate solution $v \in H$, we propose that given $\epsilon > 0$ there exist $M \in \mathbf{N}$, $v^* = \sum_{i=1}^M a_i\psi_i \in G = G_M$, and $\delta > 0$ such that $\nabla\hat{J}(a) = 0$, $||v^* - v|| < \epsilon$, and Newton's method (continuous or discrete) converges to v^* in G given any initial approximation v_0 with $||v^* - v_0|| < \delta$. Experimentally, one uses a small step size to approximate the continuous Newton's flow

$$u'(s) = -(D^2J(u(s)))^{-1}\nabla J(u), \quad u(0) = u_0\,.$$

One might use this connection analytically to either prove an existence result from a discrete convergence result or the other way around. Multiplying by $D^2J(u(s))$ and undoing the chain rule results in the initial value problem

$$(\nabla J(u(s)))' = -\nabla J(u(s)), \quad \nabla J(u(0)) = \nabla J(u_0)\,.$$

Then $\nabla J(u(s)) = \nabla J(u_0)e^{-s}$, so that the gradient goes to zero and $u'(s) = -(D^2J(u(s)))^{-1}$

$\nabla J(u_0)e^{-s}$. If the inverse (pseudoinverse) of $D^2J(u(s))$ could be controlled, then convergence of the flow to a critical point might be proven. The fact that J satisfies the Palais–Smale condition (see [Rabinowitz, 1986] or [Castro *et al.*, 1998]) or a similar argument might be useful in showing that $\lim_{s\to\infty} u(s)$ exists. The coercivity of J (see [Castro *et al.*, 1997]) might also be appealed to. It seems reasonable that the signature should be constant along these flows, at least when the limit (solution) is nondegenerate. Perhaps the most tractable of our conjectures is that there exist initial values of arbitrarily large signature, whereby convergence along signature-invariant flows would provide the existence of infinitely many solutions.

It is well known that the basins of attraction for continuous Newton's method are more straightforward than those of discrete Newton's method, typically lacking the fractal boundaries and accompanying dynamical complexities. As in simple cases (where it can be easily proven), continuous Newton's method when applied to the variational formulation of (1) appears to have connected basins with measure zero boundary. Obviously if one could describe the basins analytically and if there were infinitely many of them, then one would have the highly desirable infinitely many solutions existence result.

Together with our Summer 1999 REU student Joel Fish, we have made some progress towards understanding these basins and their boundaries. There are simple examples where continuous Newton flows terminate in finite time to points that are not roots, e.g. where a zero derivative is encountered. The inflection sets (where $D^2J(u(s))$ is not invertible) almost certainly contain such points. The experimental and novel work of our REU student suggests that the collection of initial points that converge to such "bad points" themselves belong to the set

$$\Gamma = \{u \in H : J'(u)(e_i) = 0 \text{ for some eigenfunction } e_i \text{ of } D^2J(u(s))\},$$

which may itself be composed of infinitely many orthogonally intersecting manifolds. It appears to be the case that the inflection sets form part of the boundaries of the basins of attraction for our Newton flows, and that part of Γ forms the rest of the boundaries. Certainly it is clear that all solutions must lie in Γ, possibly at the points where infinitely many (all but one) manifolds intersect orthogonally. Degenerate solutions which belong to both an inflection set and Γ exist and add to the difficulty of finding a proof. Finally, we have experimentally observed a subset of Γ that very closely resembles the manifold S used in CCN in that it appears to be a codimension 1 submanifold diffeomorphic to the unit sphere which contains all nontrivial solutions to 1.

If everything in this section could be proven, one could infer the existence of infinitely many solutions! The authors feel this research direction shows a lot of promise but realize that parts of the argument might be very hard.

6. Conclusions and Future Efforts

We are in the process of duplicating this experiment for the case where Ω is a disk in $\mathbf{R}^2$, where much is known about radial solutions but not so much about the nonradial solutions. For that experiment, we can use the well-known basis built from Bessel functions.

All of our numerical experiments support our "zero-set conjecture", which states that the CCN solution has an internal zero set which intersects the boundary $\partial\Omega$. In particular, if proven this would imply that the MI 2 CCN solution on the disk is nonradial. When $\Omega = (0, 1) \times (0, 1)$, the solution possessing "radial symmetry" is the one corresponding to $\psi_{1,3} + \psi_{3,1}$ (see also [Costa *et al.*, 1999]). Our numerical experiment provides a MI greater than 2, confirming that this is not the CCN solution. Using generic eigenfunction generating code for arbitrary regions in the plane, it should be possible to repeat this experiment for annuli, triangles, dumb-bells and other interesting shapes where unlike the square (sine functions) and the disk (Bessel functions), the eigenfunctions may not be known in closed form. Some doubt has been expressed that these experiments will be entirely successful, as accurate eigenfunction generation is often difficult. It is our belief that all important qualitative features will be revealed by our method even in those cases, though of course accuracy of approximation will be limited by the accuracy of the basis representation. It should be pointed out that the eigenfunctions of $-\Delta$ make an excellent choice as a basis for our elliptic problems since they are intrinsically related to solutions, but they are not the only choice. In theory, any orthonormal basis could be used, as long as one had reason to be confident that, once ordered,

the solutions depended heavily on the first finitely few and not so much on the remaining infinitely many. For our problem one does indeed observe that the coefficients of the higher modes become quite small, giving such confidence.

An interesting problem to try with the GNGA method that makes clear the potential to solve problems other than elliptic superlinear ones is the simple ODE $y' = y$ on $\Omega = (-1, 1)$. Using a basis of normalized Legendre polynomials and the functional

$$J(w) = \int_\Omega (w' - w + c)^2 \, dx, \quad w(0) = 0$$

one gets immediate convergence to $y - c = w$ since J is quadratic and hence the function $\nabla J(w)$ one is applying Newton's method to is linear. It seems worth pursuing the applicability of GNGA to a very wide class of variational problems, e.g. any problem where

1. One has a functional whose critical points are the desired solutions.
2. One has an orthonormal basis for the function space the solutions lie in.
3. One knows that the solutions depend most heavily on the lower modes.

Certainly we can apply this method to many elliptic problems with varying boundary conditions. We believe that we can also apply the method to hyperbolic and even parabolic problems. Since our interest is primarily in proving existence theorems in elliptic PDE, we are hopeful that GNGA will be useful in providing insight (such as the MI of solutions) and may be of direct use in proving such theorems by analyzing the continuous Newton Flow.

References

Adams, R. [1975] *Sobolev Spaces* (Academic Press, NY).

Argyros, I. K. [1999] "The asymptotic mesh independence principal for inexact Newton–Galerkin-like methods," *Pure Math. Appl.* **8** (2–4), 169–194.

Castro, A. & Kurepa, A. [1987] "Infinitely many radially symmetric solutions to a superlinear Dirichlet problem in a ball," *Proc. AMS* **101**, 57–64.

Castro, A., Cossio, J. & Neuberger, J. M. [1997a] *Sign-Changing Solutions for a Superlinear Dirichlet Problem* (Rocky Mountain J. M).

Castro, A., Cossio, J. & Neuberger, J. M. [1997b] "On multiple solutions of a nonlinear Dirichlet problem," *Proc. Second World Congress of Nonlinear Analysts*, Part 6 (Athens, 1996); *Nonlin. Anal.* **30**(6), 3657–3662.

Castro, A., Cossio, J. & Neuberger, J. M. [1998] "A min-max principle, index of the critical point, and existence of sign-changing solutions to elliptic boundary value problems," *Electron. J. Diff. Eqs.* **2**, 1–18.

Choi, Y. S. & McKenna, P. J. [1993] "A mountain pass method for the numerical solutions of semilinear elliptic problems," *Nonlin. Anal.* **20**, 417–437.

Chow, S. N. & Hale, J. K. [1982] *Methods of Bifurcation Theory* (Springer-Verlag, Berlin, NY).

Costa, D., Ding, Z. & Neuberger, J. M. [1999] "A numerical investigation of sign-changing solutions to superlinear elliptic equations on symmetric domains," *J. Comp. Appl. Math.*, to appear.

Crawford, J. D., Golubitsky, M., Gomes, M. G. M., Knobloch, E. & Stewart, I. N. [1991] *Boundary Conditions as Symmetry Constraints*, Lecture Notes in Mathematics **1463**, pp. 63–79.

Kinderlehrer, D. & Stampacchia, G. [1979] *Introduction to Variational Inequalities and Their Applications* (Academic Press, NY).

Gilbarg, D. & Trudinger, N. [1983] *Elliptic Partial Differential Equations of Second Order* (Springer-Verlag, Berlin, NY).

Golubitsky, M., Stewart, I. N. & Schaeffer, D. G. [1988] *Singularities and Groups in Bifurcation Theory, Vol. II*, Applied Mathematical Sciences **69** (Springer-Verlag, NY, Berlin, Heidelberg).

Gomes, M. G. M. & Stewart, I. N. [1994] "Steady PDEs on generalized rectangles: A change of genericity in mode interactions," *Nonlinearity* **7**, 253–272.

Gomes, M. G. M., Labouriau, I. S. & Pinho, E. M. [1999] "Spatial hidden symmetries in pattern formation," *Pattern Formation in Continuous and Coupled Systems, IMA Vol. Math. Appl.* **115** (Springer, NY), pp. 83–99.

Johnson, L. & Riess, R. [1982] *Numerical Analysis* (Addison-Wesley, Reading, MA).

Ljusternik, L. & Schnirelmann, L. [1934] *Methodes Topologique dans les Problems Variational* (Hermann and Cie, Paris).

Milnor, J. [1963] *Morse Theory* (Princeton University Press, Princeton).

Neuberger, J. W. [1988] "Constructive variational methods for differential equations," *Num. Anal. Th. Meth. Appl.* **13**(4), 413–428.

Neuberger, J. M. [1997a] "A numerical method for finding sign-changing solutions of superlinear Dirichlet problems," *Nonlin. World* **4**(1), 73–83.

Neuberger, J. W. [1997b] *Sobolev Gradients and Differential Equations*, Springer Lecture Notes.

Neuberger, J. M. [1998] "A sign-changing solution for a superlinear Dirichlet problem with a reaction term nonzero at zero," *Nonlin. Anal.* **33**(5), 427–441.

Rabinowitz, P. [1986] *Minimax Methods in Critical Point Theory with Applications to Differential Equations*, Regional Conf. Series in Mathematics **65** (AMS, Providence, RI).

Tehrani, H. [1996] "H^1 versus C^1 local minimizers on manifolds," *Nonlin. Anal.* **26**(9), 1491–1509.

Wang, Z. Q. [1991] "On a superlinear elliptic equation," *Ann. Inst. H. Poincare Analyse Non Lineaire* **8**, 43–57.